Sunitinib inhibits tumor growth and synergizes with cisplatin in orthotopic models of cisplatin-sensitive and resistant human testicular germ cell tumors

Running title: Effect of sunitinib in orthotopic testicular GCT

W. Castillo-Ávila[1], J.M. Piulats[1,2], X. Garcia del Muro[2], A. Vidal[3], E. Condom[3], O. Casanovas[1], J. Mora[4], J.R. Germà[2], G. Capellà[1], A. Villanueva[1] & F. Viñals[1,5 *]

1 Laboratori de Recerca Translacional and 2 Servei d'Oncologia Mèdica, Institut Català d'Oncologia-IDIBELL, Hospital Duran i Reynals, L'Hospitalet de Llobregat; 3 Servei d'Anatomia Patològica, Hospital Universitari de Bellvitge-IDIBELL; 4 Departament de Bioquímica, Hospital de Sant Pau; Barcelona 5 Departament de Ciències Fisiològiques II, Universitat de Barcelona-IDIBELL, L'Hospitalet de Llobregat

Key words: Sunitinib, testicular germ-cell tumors, angiogenesis, cisplatin.

To whom correspondence should be addressed. Mailing address: Dr. Francesc Viñals - Laboratori de Recerca Translacional, Institut Català d'Oncologia- IDIBELL, Hospital Duran i Reynals, Gran Via s/n km 2,7, 08907 L'Hospitalet de Llobregat, Barcelona, Spain. E-mail: fvinyals@ico.scs.es.

WCA is a recipient of a pre-doctoral fellowship from Marató de TV3. JPR is a recipient of a fellowship from Spanish Association Against Cancer (AECC). This work was supported by research grants from Ministerio de Educación y Ciencia, Spain (Programa Ramón y Cajal, SAF2004-01350 and SAF2007-60955 to FV; SAF2002-02265 to AV), Ministerio de Sanidad y Consumo, Spain (FIS2003-PI030264 to XGM), Generalitat de Catalunya (Departament d'Universitat, Recerca i Societat de la Informació, 2005SGR00727) and Fundació La Marató de TV3 (051430 to FV and XGM).

Statement of Translational Relevance

Identifying new alternatives for the treatment of patients with testicular germ cell tumors (TGCTs) refractory to cisplatin (CDDP) chemotherapy remains a priority. In the present study we evaluated the effect of sunitinib, an oral multitarget tyrosine kinase receptor inhibitor, in a preclinical model of testicular GCTs. Our results indicate that sunitinib has antitumor activity, and that combination therapy with CDDP enhances the effect induced by either agent alone. Remarcably, sunitinib was equally effective in a CDDP-resistant model of testicular GCT. Thus our results suggest that sunitinib might constitute a new alternative for the treatment of CDDP-refractory patients. Moreover, in clinical trials with drugs as sunitinib, it would be interesting to continue the CDDP treatment even after development of drug resistance has taken place.

Abstract

Purpose: Germ cell tumors (GCTs) of the testis are highly curable, but those patients who are refractory to cisplatin (CDDP)-based combination chemotherapy have a poor prognosis. Therefore, identifying new alternatives for treatment remains a priority. Several studies support an important role for angiogenesis in GCTs, suggesting antiangiogenic treatment might be a good alternative. Sunitinib is an oral multitarget tyrosine kinase receptor inhibitor with antiangiogenic and antitumor activities. In the present study, we evaluated the effect of sunitinib, CDDP or the combination of both drugs using an orthotopic model of human testicular GCT.

Experimental Design: Mice were implanted with 4 different testicular tumors: a yolk sac, two choriocarcinomas and finally a CDDP-resistant choriocarcinoma variant induced in mice by continuous exposure to CDDP. Mice were treated with vehicle, CDDP, sunitinib or the combination of both drugs and their effects on tumors were analyzed.

Results: We observed a significant inhibition in tumor growth accompanied by longer survival after sunitinib treatment. Combination therapy with CDDP significantly enhanced these effects. Sunitinib induced apoptosis, reduced tumor cell proliferation and tumor vasculature, and inhibited VEGFR-1, -2 and -3, and PDGFRα phosphorylation without affecting phosphorylation of other tyrosine kinase receptors. More importantly, tumor growth inhibition induced by sunitinib was also observed in the induced CDDP-resistant choriocarcinoma model.

Conclusions: Taken together, these results suggest that sunitinib might be a new alternative for treatment of CDDP-refractory patients.

Introduction

Germ cell tumors (GCTs) of the testis are the most common solid tumors in men aged 15-35 years and represent 95% of tumors arising in the testes. Testicular GCTs can be classified as seminoma or non-seminoma according to their histological characteristics. Each group represents approximately 50% of GCTs. Non-seminoma tumors include embryonal cell carcinoma, yolk sac tumor, choriocarcinoma and teratoma. Most non-seminoma tumors are composed of two or more of these cell types; seminoma may also be a component (1).

GCTs are highly curable even in patients with metastatic disease. Approximately 70-80% of patients with metastatic germ cell cancer can be cured after cisplatin (cis-dichlorodiammine platinum or CDDP) based combination chemotherapy, such as BEP (bleomycin, etoposide and cisplatin) or VIP (etoposide, ifosfamide and cisplatin) (2); however, resistance to cisplatin treatment may arise. Indeed, two different types of resistance are observed: cisplatin-refractory disease which consists in disease stabilization during treatment followed by disease progression within 4 weeks after cisplatin-based chemotherapy and absolute cisplatin-refractory disease in which there is disease progression even during treatment (3). Patients refractory to cisplatin-based combination chemotherapy have a poor prognosis. The identification of new treatment alternatives for patients with refractory disease remains a priority and novel molecular targets are being explored.

Antiangiogenic therapy has the potential to be an effective strategy for human cancer treatment. Angiogenesis, or the formation of new blood vessels from pre-existing vasculature, is a complex multistep process that includes endothelial cell proliferation, vessel sprouting, vascular permeability and the remodelling and maturation of emerging vessels. Angiogenesis is essential to support the growth and metastatic dissemination of

most solid tumors (4, 5). A balance between pro-angiogenic and anti-angiogenic factors controls this process. Multiple growth factors, including vascular endothelial growth factors (VEGFs), fibroblast growth factors (FGFs) and plateled-derived growth factors (PDGFs), exert an important pro-angiogenic effect through binding of specific cell-surface receptor tyrosine kinases (RTKs) (6). In addition to ligand activation, somatic mutations also can activate RTKs. Enhanced activity of many RTKs has been implicated in tumor growth, progression, metastasis and angiogenesis (7).

Sunitinib is an oral multitarget RTK inhibitor with antiangiogenic and antitumor activities. Sunitinib inhibits RTKs expressed by tumor cells and involved in tumor proliferation and survival, including stem cell factor receptor (c-Kit), Fms-like tyrosine kinase 3 (FLT3), colony stimulating factor type I receptor (CSF-1) and the glial cell line derived neurotrophic factor receptor (RET) (8, 9). Moreover, sunitinib inhibits RTKs expressed on endothelial and mural cells, such as platelet-derived growth factor receptor (PDGFR-α and PDGFR-β) and vascular endothelial growth factor receptor (VEGFR types 1 and 2), which are involved in angiogenesis (8, 10). The antitumor activity of sunitinib has been demonstrated in preclinical and clinical studies. Tumor regression has been shown in different xenograft models of colon cancer, breast cancer, non-small-cell lung cancer, melanoma, glioblastoma, renal carcinoma and epidermal cancer (10-12). Clinically, sunitinib antitumor activity has been demonstrated in phase I, II and III trials in patients with renal cancer, gastrointestinal stromal tumors (GIST), breast cancer, neuroendocrine tumors, colorectal cancer, sarcoma, thyroid cancer, melanoma and non-small-cell lung cancer (11-15). In addition, sunitinib received United States Food and Drug Administration approval in January 2006 and European Union approval in January 2007 for treatment of advanced renal cell carcinoma and patients with GIST who are refractory or intolerant to imatinib (16, 17).

Several reports have shown that some of the RTKs inhibited by sunitinib and their specific ligands are implicated in the development of human testicular GCTs, like c-Kit, PDGFRs or VEGFRs (18-20). In the present study, we evaluated the effect of sunitinib on a newly developed model of human testicular GCTs orthotopically grown in nude mice. We used 4 different tumors types including yolk sac and choriocarcinoma. Because platinum-based drugs are the standard treatment for GCTs, we evaluated the antitumor and antiangiogenic activity of sunitinib alone or in combination with CDDP. Our results indicate that sunitinib clearly inhibited tumor growth, prolonged mice survival and reduced tumor vasculature. More interestingly, sunitinib was equally effective in a CDDP-resistant model of testicular GCT, suggesting that this drug might be a new alternative for treatment of CDDP-refractory patients.

Materials and Methods

Chemical compounds

Sunitinib was kindly provided by Pfizer (New York, USA) and was dissolved in carboxymethylcellulose (CMC) solution (CMC 0.5%, NaCl 1.8%, Tween 80 0.4% and benzyl alcohol 0.9% in distilled water) and adjusted to pH 6.0. Drug aliquots were prepared once weekly and kept in the dark at 4ºC. CDDP was diluted in sterile serum before i.p injection. All other reagents were from Sigma (ST. Louis, MO) unless stated otherwise.

Orthotopic implantation of testicular tumors

Male nu/nu Swiss mice were purchased from Charles River (Wilmington, MA). Mice were housed and maintained in laminar flow cabinets under specific pathogen-free conditions. All the animal studies were approved by the local committee for animal care.

Fresh surgical specimens of GCTs of the testis were obtained after surgical resection from the Hospital Universitari de Bellvitge (L'Hospitalet de Llobregat) and Fundació Puigvert (Barcelona, Spain) and placed in DMEM media (Biowhittaker) supplemented with 10% FCS, 50 units/ml penicilin and 50 μg/ml streptomycin sulfate. Testicular human germ cell tumors were minced and two pieces of each tumor were orthotopically implanted. Briefly, five-week old male weighing 18-22 g were anesthetized by isofluorane inhalation. A small midline incision was made and the testes were exteriorised. A piece of tumor was then implanted on each testis using prolene 7-0 surgical sutures. The testes were returned to the abdominal cavity and the incision was closed with wound clips. Different tumors were perpetuated in mice by consecutive passages (at least six) according to the growth rate of each tumor type: when an intra-

abdominal mass was palpated testes and tumors were exteriorised and a piece of tumor (2-5 mm^3) was then implanted on testis of a new animal as described before for the primary tumor. Only non seminoma tumors (mainly choriocarcinomas, embryonal carcinoma, yolk sac or mixtures) were perpetuated in mice; all pure seminomas present as primary tumors failed to grow as xenografts.

For our studies with sunitinib we use four models of pure non seminoma GCTs of the testis: a yolk sac (TGT1); two choriocarcinomas (TGT17 and TGT38); and finally the CDDP-resistant variant of one of the choriocarcinomas (TGT38R) which was developed by continuous exposure of mice to CDDP and shows acquired resistance to this drug.

Treatment Schedule

Approximately ten days after tumor implantation in the case of TGT17, TGT38 and TGT38R choriocarcinomas, and 30 days after tumor implantation in the case of TGT1 yolk sac tumor, a palpable intra-abdominal mass was detected. Presence of tumor was posteriorly confirmed by detection of high serum levels of human alpha-fetoprotein (for yolk sac tumors) and human chorionic gonadotropin (for choriocarcinomas), two surrogate markers for these tumors (see later). In this moment, mice were randomized into four treatment groups (n= 10 mice/group in TGT17 choriocarcinoma; n= 7 mice/group in TGT38 and TGT38R choriocarcinomas; n= 5 mice/group in TGT1): a) daily oral administration of sunitinib vehicle solution (carboxymethylcellulose suspension) for 15 days and intraperitoneal (i.p.) administration of 3 doses of physiological serum at 5-day interval (control group); b) i.p administration of 3 doses of 2 mg/kg of CDDP at 5-day intervals (CDDP group); c) daily oral administration of 40 mg/kg of sunitinib for 15 days (sunitinib group); and d) i.p administration of 3 doses of 2 mg/kg of CDDP at 5-day intervals and daily oral administration of 40 mg/kg of

sunitinib for 15 days (CDDP and sunitinib group). The chosen doses of 40 mg/kg of sunitinib and 2 mg/kg of CDDP were found to be the most effective in mice in previous studies (10).

Studies were finished when tumors in vehicle-treated animals were judged to adversely affect their well being (20-25 days after tumor implantation for mice bearing choriocarcinoma tumors, and 65-70 days for mice bearing yolk sac tumors). Mice were sacrificed by cervical dislocation and the effect of the different treatments on tumor response was evaluated by tumor volume: volume= (length)(width^2 /2).

For determination of survival time and establishment of Kaplan-Meier survival curves, mice bearing TGT17 choriocarcinoma were treated with vehicle, 40 mg/kg of sunitinib for 15 days, 3 doses of 2 mg/kg of CDDP at 5-day intervals and the combination of both drugs (5 mice/group). Animals were sacrificed when tumors were judged to affect their well being.

Quantification of circulating tumor markers

Serum levels of Alpha-fetoprotein (AFP) (for yolk sac tumors) and the β-subunit of human chorionic gonadotropin (β-hCG) (for choriocarcinomas) are used as surrogate markers of tumor burden (2, 21, 22). They were measured in nude mice serum using commercially available two-site enzyme chemiluminometric assays automated on the Immulite®-2000 analyzer. AFP assay uses beads coated with monoclonal murine anti-AFP and alkaline phosphatase conjugated to polyclonal rabbit anti-AFP (23). β-HCG assay uses beads coated with monoclonal murine anti-β-HCG and alkaline phosphatase conjugated to polyclonal ovine anti- β-HCG (24). Reactions were linear up to 300 KU/L for AFP and up to 5000 U/L for β-HCG. Higher concentrations were diluted with the corresponding provided diluents. Assay sensitivity was 0.2 KU/L and 0.4 U/L for AFP

and β-HCG, respectively. Reference values of $\leq$ 9 KU/L for AFP and $\leq$ 5 U/L for β-HCG were established based on healthy controls.

Histological studies

Part of the tumor from control or treated mice was formalin-fixed and paraffin-embedded, while another part was embedded in OCT compound and stored at -80ºC. Paraffin-embedded tissues were used to visualize general tissue morphology by H&E staining and to detect c-kit expression by immunohistochemical staining using a 1:50 dilution of rabbit anti-c-kit antibody (Dako, Denmark). The immunostained sections were counterstained using hematoxylin.

OCT-frozen sections were used for immunofluorescence staining. Double immunofluorescence staining was performed to detect CD31/Desmin, CD31/Ki67, CD31/activated caspase-3 and PDGFR-α/Desmin expression. Sections were incubated overnight at 4ºC with a 1:50 dilution of rat monoclonal antibody for CD31 (BD PharMingen, San Diego, CA) and either a 1:500 dilution of rabbit antibody for Desmin (NeoMarkers, Fremont, CA), a 1:100 dilution of rabbit antibody for Ki67 (NeoMarkers, Fremont, CA) or a dilution 1:500 of rabbit antibody for activated caspase-3 (Cell Signalling, MA). For double immunofluorescence staining of PDGFRα/Desmin, sections were incubated overnight at 4ºC with a 1:100 dilution of rat antibody for PDGFRα (eBioscience, San Diego, CA) and a 1:500 dilution of rabbit antibody for Desmin. Sections were washed twice with PBS and incubated with a 1:300 dilution of Alexa Fluor 488 conjugated goat anti-rabbit plus a 1:200 dilution of Alexa Fluor 546 conjugated goat anti-rat (Molecular Probes, Eugene, OR) at room temperature for 1h in the dark. The slides were then washed twice in PBS and incubated with a 1:1000 dilution of TO-PRO-3 (Molecular Probes) for 10 minutes in the dark. Finally, the slides

were washed twice in PBS and coverslips were mounted using Gel Mount aqueous mounting medium (Sigma Chemical, ST. Louis, MO).

To identify apoptotic cells, terminal deoxynucleotidyl transferase biotin-dUTP nick end labelling (TUNEL) staining (Promega, Mannheim, Germany) was used, following the manufacturer's protocol. Briefly, after incubation of samples with equilibration buffer for 5-10 minutes at room temperature, sections were incubated with rTdT reaction mix at 37ºC for 1 hour inside a humidified chamber. Then, samples were washed with 2X SSC and PBS, and incubated with a 1:50 dilution of rat anti-mouse monoclonal antibody for CD31 (BD PharMingen, San Diego, CA). Sections were washed twice with PBS and incubated with a 1:500 dilution of Streptavidine 488 FITCH and a 1:200 dilution of Alexa Fluor 546 conjugated goat anti-rat (Molecular Probes, Eugene, OR) for 1 hour at room temperature. Finally, samples were incubated with a 1:1000 dilution of TO-PRO-3 for 10 minutes in the dark.

Images of sections were obtained on a Leica TCS SL spectral confocal microscope. To quantify CD31, Ki67 and TUNEL staining, five hot spot fields in viable tissue zones at x400 magnification were captured for each tumor. Quantification of staining areas was performed using ImageJ software.

RTK array analysis

To determine which tyrosine kinase receptors were targeted by sunitinib, a human Phospho-RTK Array C-Kit (R&D Systems, Minneapolis, MN, USA) was used to detect the tyrosine phosphorylation levels of 42 different RTKs. Mice bearing TGT38 choriocarcinoma were treated with sunitinib (40 mg/kg) or vehicle alone for 15 days. Mice were sacrificed 4 hours after the last dose. Tumor samples obtained from 4 control and 4 sunitinib-treated mice were mechanically disrupted using lysis buffer (1% NP-40,

20 mM Tris-HCl pH 8.0, 137 mM NaCl, 10% glycerol, 2 mM EDTA, 1 mM sodium orthovanadate, 10 µg/ml aprotinin, 10 µg/ml leupeptin) and a glass homogenizer on ice. Protein concentration was determined using a BCA assay kit (Pierce Chemical Company, Rockford, IL.). RTK array analysis was performed according to the manufacturer's protocol. Array membranes were blocked and incubated with 500 µg of tumor lysate overnight at 4ºC on a rocking platform shaker. Then, the arrays were washed, incubated with anti-phosphotyrosine-HRP for 2 h at room temperature, washed again and developed with ECL Western blotting detection reagent (Amersham Pharmacia Biotech, Cambridge, UK). Average pixel density of duplicate spots was determined using the Quantity One software, and values were normalized against corner duplicate phosphotyrosine-positive control spots. Results were expressed as a ratio of sunitinib treated to untreated samples.

Quantitative real-time PCR

Real-time PCR of cDNA obtained from TGT17, TGT38 and TGT1 tumors was performed with SYBR-green (Roche Molecular Biochemicals, Lewes, UK) and specific primers for human PDGFR-α (5'AGTTCCTTCATCCATTCTGGACT and 5'ACCGTCTGTCCCCCAGTT); mouse PDGFR-α (5'CAGTCCACCCGTGTGCT and 5'GAAAATTCAACAGCAGCTGGT); human PDGFR-β (5'CATCACCGTGGTTGAGAGC and 5'AATTGTAGTGTGCCCACCTCTC); mouse PDGFR-β (5'CAGTGACAGACTACCTCTTTGGAG and 5'GATATGCAGGATGGAGCCA); human VEGFR-2 (5'TGTACGGTCTATGCCATTCCT and 5'GGGTATGGGTTTGTCACTGAG); mouse VEGFR-2 (5'AGCGGAGACGCTCTTCATAA and GTGCCGACGAGGATAATGAC); and the house keeping genes human β-actin (5'GAGGCAGCCAGGGCTTA and 5'AACTAAGGTGTGCACTTTTATTCAACT)

and mouse β-actin (5'GGGGGTTGAGGTGTTGAG and 5'GTCTCAAGTCAGTGTACAGGCC) designed using the Primer3 software. Real-time PCR was run on a LightCycler instrument (Roche Molecular Biochemicals, Lewes, UK). Forty cycles of amplification with denaturation at 95ºC for 10 seconds, followed by annealing at 65ºC for 20 seconds and extension at 72ºC for 13 seconds, were performed after an initial incubation at 95ºC for 10 minutes. The dC_t values were calculated after subtracting the mean C_t values of β-actin gene from the PDGFR-α mean C_t values.

Statistical Analyses

Statistical significance of differences in tumor growth and in TUNEL, CD31 and Ki67 expression between control and treated tumors was determined using the Mann-Withney U-test. The log-rank test was performed to compare survival curves from the different treatment groups. In all experiments, differences were considered statistically significant when $p < 0.05$.

Results

Sunitinib induces inhibition of tumor growth in testicular orthotopic models and sinergizes with CDDP.

Our aim was to evaluate antiangiogenic therapy as an alternative to CDDP in testicular germ cell tumors. For this, we used new orthotopic models of human testicular GCT recently developed in our laboratory; these models, all of them generated from non seminoma human GCTs, have been shown to accurately reproduce the histological and genetic characteristics of these testicular GCTs, as well as their response to CDDP (Piulats et al., manuscript submitted). We used three different orthotopic GCTs of the testis chosen because of their belonging solely to a specific hystological type: a yolk sac (TGT1) and two choriocarcinomas (TGT17 and TGT38). First, we analyzed the angiogenic pattern and the expression of several proangiogenic RTKs in these tumors. Orthotopic GCTs were highly vascularized, presenting high vessel density positive for CD31 (an endothelial marker) but also for desmin (a perycite marker) (Fig 1A). Concerning RTKs, we analyzed the mRNA expression of VEGFR2, PDGFRα, and PDGFRβ using quantitative RT-PCR. We designed primers that specifically recognized human or mouse mRNA in order to discriminate between receptors expressed by human tumor cells or mouse stromal cells in our xenograft model. Thus, VEGFR2 was only expressed in the mouse endothelial compound and absent in human tumoral cells (Fig. 1B). PDGFRβ presented a similar expression profile as that of VEGFR2, being expressed only by the stromal compound of tumors. In contrast, PDGFRα was not only expressed by the mouse stromal compound but also by human tumoral cells. In order to confirm this, PDGFRα protein expression was analyzed by immunofluorescence. PDGFRα expression was detected in stromal desmin-positive mural cells but also in tumoral cells (Fig. 1C and Supplementary Fig. 1). We did not detect the expression of

other RTKs such as c-kit or Flt-3 expression in our GCT model (Supplementary Fig. 1 and data not shown). Altogether, these data suggested that a multitarget RTK inhibitor such as sunitinib, which also displays antiangiogenic activity, could be an optimal candidate for the treatment of these tumors.

Next, we examined the effect of sunitinib and CDDP on the growth of these tumors. Mice were treated with vehicle (untreated), CDDP, sunitinib or the combination of both drugs as described in the Materials and methods section. All animals were sacrificed once tumors of the control group adversely affected their well being; and the effect of the different treatments was determined by measuring tumor volume (Fig. 2A). As expected, CDDP treatment reduced tumor volume in all cases. Treatment with sunitinib as a single agent also resulted in a reduction of tumor volume compared to the control group. Combination therapy with sunitinib and CDDP enhanced the antitumor activity of these drugs inducing a significantly greater decrease in tumor volume than that observed in any of the other arms of the study. In the case of TGT17 choriocarcinoma, tumors treated with the combination of sunitinib and CDDP completely regressed.

We used circulating serum levels of β-HCG and AFP as surrogate markers of tumor burden (for choriocarcinoma and yolk sac tumors, respectively) (Fig.2B). CDDP and sunitinib, alone or in combination, reduced β-HCG and AFP levels with respect to the control group, suggesting that these treatments inhibit tumor burden.

The combination of sunitinib and CDDP increases mice survival.

To determine whether the administration of CDDP, sunitinib or their combination was able to prolong survival in animals with testicular GCTs, athymic mice bearing TGT17 choriocarcinoma were randomized into four treatment groups as described above. Mice were maintained until death for Kaplan-Meier analysis (Fig. 3).

Median survival time of control group was 13 days. CDDP and sunitinib treatment enhanced mouse survival compared to the control group (median survival times were 33 and 36 days, respectively). There were no significant differences in median survival time between both treatments. However, the co-administration of the two drugs increased the median survival compared to the controls, but also compared to single agent treatment with CDDP or sunitinib (median survival time of combined therapy was 47 days).

Sunitinib promotes apoptosis and reduces microvascular density and cell proliferation.

In order to understand the mechanisms that contribute to tumor growth inhibition induced by sunitinib, tumor sections from control or treated mice bearing TGT38 choriocarcinoma were evaluated by histological and immunohistochemical analysis. H&E staining showed significant tumor necrosis in tumors treated with CDDP alone or combined with sunitinib. Percentage of necrotic tissue was approximately 80% for tumors from CDDP treated mice and 90% for tumors from CDDP and sunitinib treated mice, whereas necrosis represented only 20% of tumor in samples from sunitinib treated mice (Fig. 4A).

Sections from tumors were further subjected to TUNEL staining to determine whether apoptosis could be involved in the reduction in tumor volume induced by the different treatments (Fig 4B). Administration of CDDP alone or in combination with sunitinib had little effect on apoptosis. However, sunitinib induced a 2.5-fold increase in apoptotic cells as compared to untreated tumors (Fig. 4C). These results were confirmed by immunodetection of activated caspase-3, an early and specific apoptotic marker. We also observed an increase in activated caspase-3 staining in sunitinib treated tumors

(Supplementary Figure 2). We then studied the possible apoptotic effect of each treatment on endothelial cells. In this case, we observed a significant increase of apoptosis in this cell type both in sunitinib treated tumors and also in tumors treated with the combined therapy (Fig. 4D).

To better understand this effect, we analyzed the effect of the different treatments on tumor vascular endothelium. CD31 endothelial marker staining was performed (Fig. 5A) and no differences in staining were observed between tumors from control or CDDP-treated mice. However, sunitinib treatment and the combination of sunitinib and CDDP resulted in a decrease of approximately 50% in CD31 expression as compared to control mice, indicating a reduction in tumor vasculature. These results are consistent with the apoptotic effect induced by sunitinib alone or in combination with CDDP on endothelial cells.

We also analyzed the effect induced by the three treatments on cell proliferation using Ki67 staining. In all cases, we observed lower Ki67 levels in tumors from treated mice than in those from tumors controls, indicating a decrease in cell proliferation (Fig. 5A).

Sunitinib inhibits RTKs involved in angiogenesis and tumor growth.

In order to determine which receptors were being targeted by sunitinib in our model, we used a human phospho-RTK array kit that detects the phosphorylation level of 42 different RTKs, including PDGF and VEGF receptors. Mice bearing TGT38 choriocarcinoma treated with vehicle or sunitinib for 2 weeks were treated with vehicle or sunitinib for an additional 4 hours. Animals were then sacrificed, the tumors extracted and phosphorylation levels of different RTKs were analyzed (Fig. 5B). It was shown that sunitinib inhibited phosphorylation of PDGFR-α and VEGFR-1, -2 and –3. However, inhibition of PDGFR-β (which has also been described as a sunitinib target)

or non sunitinib-target receptors (such as EGF receptors) was not observed. These results suggested that sunitinib could also be exerting a direct effect on tumor cells.

Effect of sunitinib on a CDDP resistant model of testicular germ cell tumor.

As mentioned before, a small proportion of patients diagnosed with GCTs are refractory to standard treatment with CDDP. Since our previous results indicated that sunitinib inhibited tumoral growth by mechanisms other than those of CDDP, we analyzed the effect of sunitinib treatment on a CDDP-resistant model. We used mice bearing TGT38R choriocarcinoma, a variant of TGT38 choriocarcinoma induced by continuous exposure of mice to CDDP which displays acquired resistance to this drug (Piulats et al., manuscript submitted and Fig. 6B). Mice treated with vehicle, CDDP, sunitinib or their combination were sacrificed when moribund and H&E staining and tumor volume determination were performed. H&E staining showed significant tumor necrosis only in tumors treated with CDDP in combination with sunitinib (Fig. 6A). As expected, there were no significant differences in tumor volume between control and CDDP treated mice. However, sunitinib treatment alone induced a significant reduction in tumor volume; the effect induced by the combination with CDDP was of similar magnitude, suggesting that CDDP does not further improve the effect of sunitinib (Fig. 6B).

Discussion

Angiogenesis has recently arised as an interesting therapeutic target to explore in testicular GCTs. Serum levels of key tumor-derived proangiogenic factors such as vascular endothelial growth factor (VEGF), basic fibroblast growth factor (bFGF) and platelet-derived growth factor (PDGF) are increased in patients with testicular GCTs (25, 26); increased expression of VEGF has also been associated with metastatic disease in GCTs (27). Moreover, many RTKs known to play an important role in angiogenesis, such as VEGFR-2 and PDGFRs, have also been implicated in the pathogenesis of testicular GCTs (28). Our data using newly developed preclinical orthotopic models of non-seminomatous human testicular GCTs confirm that these tumors are highly vascularized and express many RTKs implicated in angiogenesis. Therefore, we have shown that these new orthotopic GCT models are a useful tool to evaluate antiangiogenic compounds.

Sunitinib is a small multitarget RTK inhibitor with antitumor activity exerted through both its antiproliferative and its antiangiogenic effect. The antiproliferative effect of sunitinib has been previously described in several human cancer cell lines and human xenograft models including renal, breast, lung, melanoma, glioblastoma and epidermoid carcinoma (8-10, 12). Thus, we assayed the effect of sunitinib in our preclinical orthotopic models of non-seminomatous testicular GCTs. Our results show that sunitinib as a single agent inhibits tumor growth in different types of testicular GCTs, including choriocarcinoma and yolk sac tumors, by inducing apoptosis and inhibiting cell proliferation. Furthermore, we observed a reduction of approximately 50% in tumor microvessel density in sunitinib-treated tumors. These results confirm the effect observed in previous reports describing the antiangiogenic activity of sunitinib. Previous *in vitro* studies show that sunitinib inhibits proliferation and migration of

human umbilical vein endothelial cells (HUVEC) and reduces capillary-like tubule formation (29). Antiangiogenic activity has also been demonstrated *in vivo*: sunitinib has been shown to reduce microvessel density in an orthotopic model of glioblastoma and also to prevent neovascularization in a tumor vascular-window model (9, 12, 21).

Multitarget agents are directed against several cancer-specific molecular targets. In our model, we show that sunitinib inhibits VEGF and PDGFR-α receptors. We believe that the antiangiogenic effect induced by sunitinib is due to inhibition of endothelial cell receptors, but also to inhibition of PDGFR-α expressed on mural cells that support tumor vasculature. However, our results suggest that in addition to this antiangiogenic activity, sunitinib could also exert its antitumor effect through a direct inhibition of PDGFR-α expressed on tumor cells. Several reports describe the antitumor effect induced by targeting tumor PDGFRs, as in the case of imatinib, a drug that inhibits tumor growth and leads to apoptosis by selective inhibition of PDGFR in some cancer models (30, 31). But more interestingly, previous reports have demonstrated that the antitumor effect induced by inhibition of PDGFRs is enhanced by simultaneously inhibiting VEGFRs, suggesting the importance of the inhibition of both PDGFRs and VEGFRs for antitumor activity (31, 32). Moreover, the antitumor effect induced by the combination of two independent agents that inhibit PDGFRs and VEGFR is similar to that observed with sunitinib treatment alone (31). These results are consistent with the potent antitumor effect induced by sunitinib in our models, where we demonstrate simultaneous inhibition of VEGF and PDGF receptors. In fact, a Phase II study of testicular GCTs aiming to determine the activity of imatinib in chemorefractory patients failed to detect any significant antitumor effect (33, 34). The results described above suggest that sunitinib could be an interesting alternative for these patients due to its simultaneous inhibition of PDGFRs and VEGFRs.

Targeted therapies are often useful in combination with standard chemotherapy because their mechanisms of action and cellular targets are often different and do not overlap. Since CDDP-based chemotherapy is the standard treatment for patients with GCTs of the testis, we analyzed the effect induced by CDDP alone or in combination with sunitinib in the different orthotopic models of testicular GCTs used in this study. There were no significant differences between the effect of sunitinib and that of CDDP on tumor growth inhibition and survival. However, a synergistic effect was observed with the combination of both drugs, confirming that their effects are exerted through different mechanisms: while CDDP is a cytotoxic agent that induces DNA damage resulting in a very high percentage of necrosis, sunitinib induces apoptosis through inhibition of several RTKs involved in tumor growth and survival. Furthermore, sunitinib also displayed antiangiogenic activity whereas CDDP treatment did not appear to have any effect on tumor vasculature. Our results are consistent with previous reports that show the synergistic effect of sunitinib with CDDP-based chemotherapy in a small cell lung cancer xenograft model (9) and with other chemotherapeutic agents such as docetaxel, 5-Fluorouracil or doxorubicin in breast cancer models (35). In all cases, the effect of combined therapy was greater than the effect induced by single agents.

GCTs are highly sensitive to chemotherapy and respond well to cisplatin-based treatment. However, approximately 15-20% of patients with metastatic non-seminomas are refractory to this treatment and have a poor prognosis. New treatment alternatives for these patients are necessary. A large number of chemotherapeutic agents, such as gemcitabine, temozolomide, irinotecan or oxaliplatin, have been evaluated in CDDP-refractory testicular GCT patients, but only partial and transient clinical activity could be demonstrated for the majority of these agents (33, 36). Taking into account all the different mechanisms of tumor growth inhibition previously described for CDDP and

sunitinib, we analyzed the effect of sunitinib on a CDDP-resistant model of testicular GCT. Our results show that sunitinib also inhibited tumor growth in this CDDP-resistant model, indicating that sunitinib can exert its antitumor effect unaffected by the CDDP-resistant phenotype. Moreover, the effect appeared to be greater than in the non resistant model (compare sunitinib effect in Fig. 2 in TGT38 with that obtained in Fig. 6 in TGT38R). Combination of both drugs caused significant tumor necrosis in CDDP-resistant tumors, absent when these tumors were treated with CDDP or sunitinib alone (Fig. 6), confirming that the combination of both drugs presents a synergistic, enhanced effect. Put together, our results from our preclinical models suggest that it could be interesting to maintain CDDP treatment in clinical trials even after development of drug resistance has taken place.

In conclusion, our results demonstrate that sunitinib as a single agent has antitumor and antiangiogenic activity in preclinical models of testicular GCTs. In addition, the administration of sunitinib in combination with CDDP enhances the effect induced by either agent alone, demonstrating the benefits of combined therapy using two drugs with different mechanisms of action. Finally, sunitinib also exhibits a potent effect on a CDDP-resistant model. Therefore, sunitinib arises as a promising novel therapeutic alternative for this disease, even in CDDP-refractory testicular GCT patients.

Acknowledgments

We thank Benjamín Torrejón (Serveis Científico-Tècnics de la Universitat de Barcelona) and Carmen Bleda (Servei de Farmàcia, Institut Català d'Oncologia, Hospital Duran i Reynals, L'Hospitalet de Llobregat) for technical support, and to James Christensen (Pfizer) for helpful suggestions.

Bibliography

1. Carver BS, Sheinfeld J. Germ Cell tumors of the testis. Ann Surg Oncol 2005;11:1-10.
2. Feldman DR, Bosl GJ, Sheinfeld J & Motzer RJ. Medical treatment of advanced testicular cancer. JAMA 2008; 299: 672-84.
3. Beyer J, Kramar A, Mandanas R et al. High-dose chemotherapy as salvage treatment in germ cell tumors: a multivariate analysis of prognostic variables. J Clin oncol 1996;14:2638-45.
4. Folkman J. Tumor angiogenesis: therapeutic implications. N Engl J Med 1971; 285:1182-6.
5. Carmeliet P. Angiogenesis in life, disease and medicine. Nature 2005;438: 932-36.
6. Shuhardja A, Hoffman H. Role of growth factors and their receptors on proliferation of microvascular endothelial cells. Microsc Res Tech 2003;60:70-5.
7. Arora A, Scholar EM. Role of tyrosine kinase inhibitors in cancer therapy. J Pharmacol Exp Ther 2005;315(3):971-9.
8. Abrams TJ, Lee LB, Murray LJ, Pryer NK, Cherrington JM. SU11248 inhibits C-KIT and platelet-derived growth factor receptor-β in preclinical models of human small cell lung cancer. Mol Cancer Ther 2003;2:471-8.
9. O'Farrell AM, Abrams TJ, Yuen HA, et al. SU11248 is a novel FLT3 tyrosine kinase inhibitor with potent activity in vitro and in vivo. Blood 2003;101:3597-605.
10. Mendel DB, Laird AD, Xin X et al. In vivo antitumor activity of SU11248, a novel tyrosine kinase inhibitor targeting vascular endothelial growth factor and

platelet-derived growth factor receptors: determination of a pharmacokinetic / pharmacodynamic relationship. Clin Cancer Res 2003;9:327-37.

11. Prenen H, Cools J, Mentens N, et al. Efficacy of the kinase inhibitor SU11248 against gastrointestinal stromal tumor mutants refractory to imatinib mesylate. Clin Cancer Res 2006;12:2622-27.
12. Boüard S, Herlin P, Christensen, et al. Antiangiogenic and anti-invasive effects of sunitinib on experimental human glioblastoma. Neuro Oncol 2007;9:412-23.
13. Motzer RJ, Michaelson MD, Redman BG, et al. Activity of SU11248, a multitargeted inhibitor of vascular endothelial growth factor receptor and platelet-derived growth factor receptor, in patients with metastatic renal cell carcinoma. J Clin Oncol 2006;24:16-24.
14. Faivre S, Delbaldo C, Vera K, et al. Safety, pharmacokinetic, and antitumor activity of SU11248, a novel oral multitarget tyrosine kinase inhibitor, in patients with cancer. J Clin Oncol 2006;24(1):25-35.
15. Chow L, Eckhardt S. Sunitinib: from rational design to clinical efficacy. J Clin Oncol 2007;25:2858-9.
16. Goodman VL, Rock EP, Dagher R, et al. Approval Summary: Sunitinib for the treatment of Imatinib refractory or intolerant gastrointestinal stromal tumors and advanced renal cell carcinoma. Clin Cancer Res 2007; 13: 1367-73.
17. Faivre S, Demetri G, Sargent W, Raymond E. Molecular basis for sunitinib efficacy and future clinical development. Nat Rev Drug Discov 2007;6: 734-45.
18. McIntyre A, Summersgill B, Grygalewicz B, et al. Amplification and overexpression of the C-KIT gene is associated with progression in the seminoma subtype of testicular germ cell tumors of adolescents and adults. Cancer Res 2005;65:8085-9.

19. Viglietto G, Romano A, Maglione D, et al. Neovascularization in human germ cell tumors correlates with a marked increase in the expression of the vascular endothelial growth factor but not the placenta-derived growth factor. Oncogene 1996;13:577-87.
20. Basciani S, Mariani S, Arizzi M, et al. Expression of platelet-derived growth factor-A (PDGF-A), PDGF-B, and PDGF receptor-alpha and -beta during human testicular development and disease. J Clin Endocrinol Metab 2002;87:2310-9.
21. Trigo JM, Tabernero JM, Paz-Ares L, et al. Tumor markers at the time of recurrence in patients with germ cell tumors. Cancer 2000;88:162-168.
22. Aparicio J, Germà JR, García del Muro X, et al. Risk-adapted management for patients with clinical stage I seminoma: The second spanish germ cell cancer cooperative group study. J Clin Oncol 2005; 23:8717-23.
23. Mora J, Gascón N, Tabernero JM, Germà JR, González F. Alpha-fetoprotein-concanavalin A binding as a marker to discriminate between germ cell tumours and liver diseases. Eur J Cancer 1995;31:2239-2242.
24. Mora J, Gascón N, Tabernero JM, Rodríguez-Espinosa J, González-Sastre F. Different hCG assays to measure ectopic hCG secretion in bladder carcinoma patients. British J Cancer 1996;74:1081-1084.
25. Bentas W, Beecken WD, Glienke W, Binder J, Schuldes H. Serum levels of basic fibroblast factor reflects disseminated disease in patients with testicular germ cell tumors. Urol Res 2003;30:390-3.
26. Aigner A, Brachmann P, Beyer J, et al. Marked increase of the growth factors pleiotrophin and fibroblast growth factor-2 in serum of testicular cancer patients. Ann Oncol 2003;14:1525-9.

27. Fukuda S, Shirahama T, Imazono Y, et al. Expression of vascular endotelial growth factor in patients with testicular germ cell tumors as an indicator of metastatic disease. Cancer 1999;85:1323-30.
28. Devouassoux-Shisheboran M, Mauduit C, Tabone E, Droz JP, Benahmed M. Growth regulatory factors and signalling proteins in testicular germ cell tumors. APMIS 2003;111:212-24.
29. Osusky KL, Hallahan DE, Fu A, Ye F, Shyr Y, Geng L. The receptor tyrosine kinase inhibitor SU11248 impedes endothelial cell migration, tubule formation, and blood vessel formation in vivo, but has little effect on existing tumor vessels. Angiogenesis 2004;7: 225-33.
30. McGary EC, Weber K, Mills L et al. Inhibition of platelet-derived growth factor-mediated proliferation of osteosarcoma cells by the novel tyrosine kinase inhibitor STI571. Clin Cancer Res 2002;8:3584-91.
31. Potapova O, Laird A, Nannini M, et al. Contribution of individual targets to the antitumor efficacy of the multitargeted receptor tyrosine kinase inhibitor SU11248. Mol Cancer Ther 2006;5:1280-88.
32. Bergers G, Song S, Meyer-Morse N, Bergsland E, Hanahan D. Benefits of targeting both pericytes and endothelial cells in the tumor vasculature with kinase inhibitors. J Clin Invest 2003;111:1287-95.
33. Piulats JM, García del Muro X, Germà JR. New Drugs in the Treatment of Germ Cell Tumors. Cancer & Chemotherapy Rev. 2007;2:232-40.
34. Einhorn LH, Brames MJ, Heinrich MC, Corless CL, Madani A. Phase II study of imatinib mesylate in chemotherapy refractory germ cell tumors expressing C-KIT. Am J Clin Oncol 2006;29:12-3.

35. Abrams TJ, Murray LJ, Pesenti E et al. Preclinical evaluation of the tyrosine kinase inhibitor SU11248 as a single agent and in combination with standard of care" therapeutic agents for the treatment of breast cancer. Mol Cancer Ther 2003;2:1011-1021.
36. Kollmannsberger C, Nochols C, Bokemeyer C. Recent advances in management of patients with platinum-refractory testicular germ cell tumors. Cancer 2006;106:1217-25.

Fig. 1 Angiogenic pattern of TGT17, TGT38 and TGT1 testicular xenograft models. A) Dual staining for the endothelial marker CD31 and the perycite marker desmin. B) Determination of VEGFR2, PDGFRα and PDGFRβ expression in TGT17 and TGT38 choriocarcinomas, and TGT1 yolk sac tumors. mRNA level of human and mouse PDGFR-α was analyzed by quantitative RT-PCR. Results are the mean of mRNA expression (4 tumors/group) $\pm$ SD and are expressed relative to human or mouse testis controls. C) Determination of tumoral and stromal expression of PDGFRα by immunofluorescence in TGT38 choriocarcinoma.

Fig. 2 Effect of sunitinib and CDDP on tumor growth in testicular xenograft models. TGT1 yolk sac and TGT17 and TGT38 choriocarcinomas were implanted orthotopically in the testis of male nude mice. Animals were treated with vehicle (untreated), 3 doses of 2 mg/kg of CDDP, 40 mg/kg of sunitinib for 15 days, or their combination (n=5 mice/group in TGT1; n= 7 mice/group in TGT17 and TGT38). A) Sunitinib and CDDP as single agents reduced tumor volume and their combination improved this effect (∗, $p < 0.05$). B) Circulating β-HCG and AFP levels detected in serum of mice bearing TGT1 yolk sac and TGT38 choriocarcinoma at different days post tumor implantation. Bars represent SD.

Fig. 3 Kaplan-Meier survival curves of sunitinib and CDDP treated mice. Mice bearing TGT17 choriocarcinoma (5 mice/group) were treated with vehicle, 3 doses of 2 mg/kg of CDDP, 40 mg/kg of sunitinib for 15 days, or the combination of both drugs. The increase in survival induced by sunitinib and CDDP treatment was enhanced by their use in combination (∗, $p < 0.05$).

Fig. 4 Histological characterization of CDDP and sunitinib-treated tumors. Mice bearing TGT38 choriocarcinoma were treated with vehicle, 3 doses of 2 mg/kg of

CDDP, 40 mg/kg of sunitinib for 15 days, or the combination of both drugs. Mice were sacrificed when control mice tumors affected the well being of the animals (20-25 days after tumor implantation, approximately) and sections from tumors were stained for H&E, CD31 and TUNEL. A) H&E staining showed increased necrosis in CDDP and CDDP+Sunitinb treated tumors whereas percentage of necrotic tissue in sunitinib treated tumors was very low. B) CD31 and TUNEL staining of viable tumor zones showed an increase in apoptosis induced by sunitinib treatment in both tumor and endothelial cells. C) Quantification of TUNEL staining was done using ImageJ software. Results are the mean $\pm$ SD of five sections of each tumor (7 tumors/treatment group) and are expressed as the percentage of positive staining for TUNEL relative to untreated group ($*$, $p < 0.05$). D) Quantification of TUNEL positive endothelial cells (CD31 positive cells). Results are the mean $\pm$ SD of five sections of each tumor (7 tumors/treatment group; $*$, $p < 0.05$).

Fig. 5 Sunitinib reduces cell proliferation and vessel density. Dual staining for Ki67 proliferation marker and CD31 endothelial marker was performed in viable zones of tumors from mice bearing TGT38 choriocarcinoma treated as in Fig. 3. CD31 and Ki67 expression was quantified using ImageJ software. Results are the mean $\pm$ SD of five sections of each tumor (7 tumors/treatment group) and are expressed as the percentage of area with positive CD31 or Ki67 staining relative to untreated group ($*$, $p < 0.05$). B) Sunitnib inhibits RTKs involved in angiogenesis and tumor growth. Mice bearing TGT38 choriocarcinoma were treated with vehicle, 40 mg/kg of sunitinib for 15 days and sacrifized 4 hours after the last dose. Tumors were resected and phosphorylation levels of different RTKs were analyzed using a human phospho-RTK array kit. Data are expressed as the ratio between the phosphorylation level of RTKs detected in sunitinib treated and untreated mice.

Fig. 6 Sunitinib inhibited tumor growth in a CDDP-resistant model of testicular germ cell tumor. Mice bearing the CDDP-resistant variant of TGT38 choriocarcinoma (TGT38R) were treated with vehicle, 3 doses of 2 mg/kg of CDDP, 40 mg/kg of sunitinib for 15 days, or their combination. Histological characterization (A) and tumor volume (B) were analyzed. A) H&E staining showed increased necrosis only in CDDP+sunitinb treated tumors, whereas percentage of necrotic tissue in CDDP or sunitinib treated tumors was very low. B) Combined therapy also improved the effect on tumor volume induced by either compound (∗, $p < 0.05$).

Supplementary Figure 1. A) Dual staining for PDGFRα and desmin in TGT17 and TGT1 tumors. PDGFRα is expressed in both tumoral and stromal compartment. B) Immunohistochemical staining was used to detect c-Kit expression in TGT1 and TGT17 primary and xenografted tumors. All tumoral cells were negative and positivity was only detected in infiltrating mastocytes.

Supplementary Figure 2. Sunitinib treatment increases activated caspase-3 expression in both endothelial and tumor cells. Dual staining for CD31 and activated caspase-3 was performed in viable zones of tumors from mice bearing TGT38 choriocarcinoma treated with vehicle, 3 doses of 2 mg/kg of CDDP, 40 mg/kg of sunitinib for 15 days, or the combination of both drugs.

Fig. 1

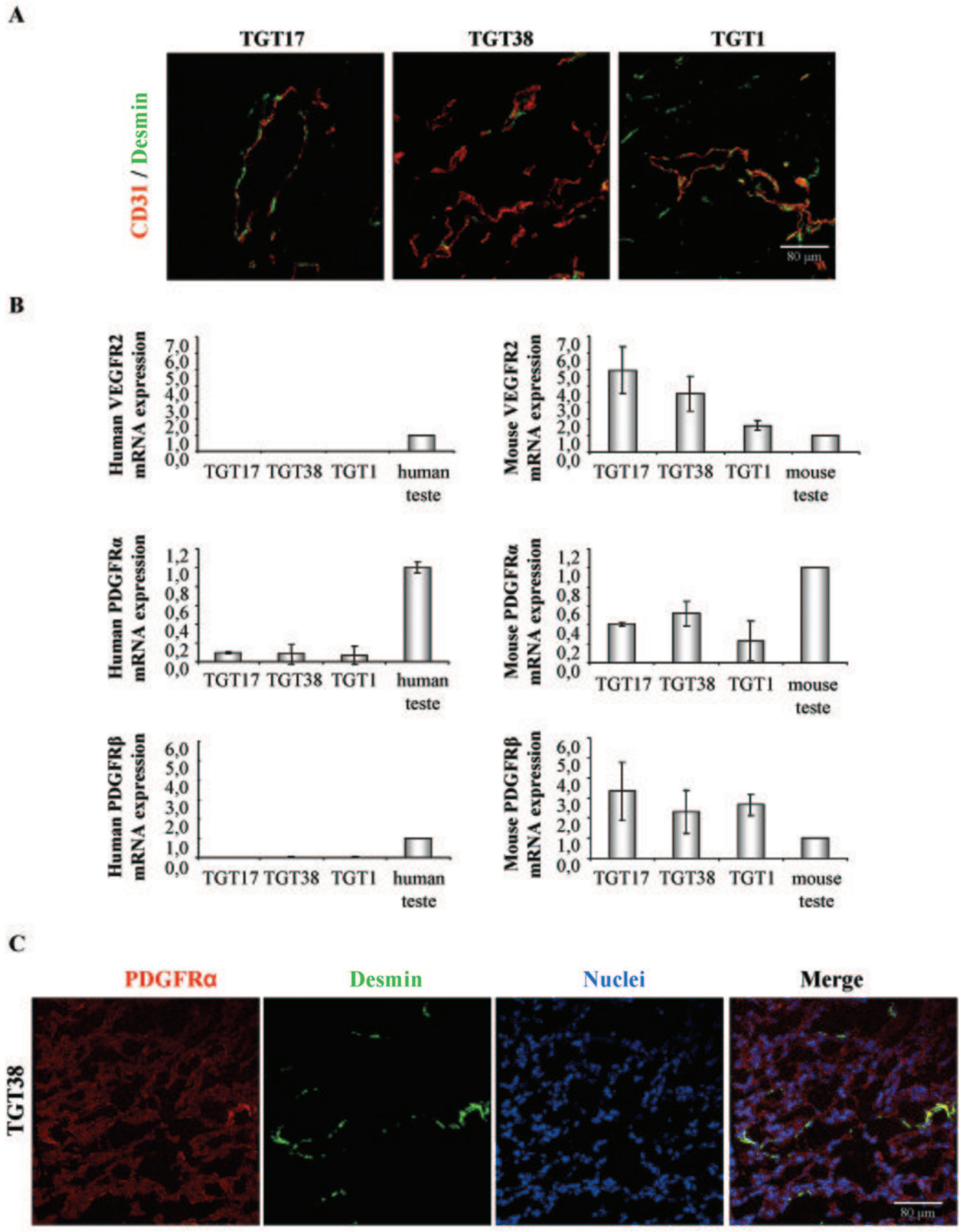
A
TGT17
TGT38
TGT1
CD31 / Desmin
80 µm
B
Human VEGFR2 mRNA expression
Mouse VEGFR2 mRNA expression
Human PDGFRα mRNA expression
Mouse PDGFRα mRNA expression
Human PDGFRβ mRNA expression
Mouse PDGFRβ mRNA expression
TGT17 TGT38 TGT1 human teste
TGT17 TGT38 TGT1 mouse teste
C
PDGFRα
Desmin
Nuclei
Merge
TGT38
80 µm

Fig. 2

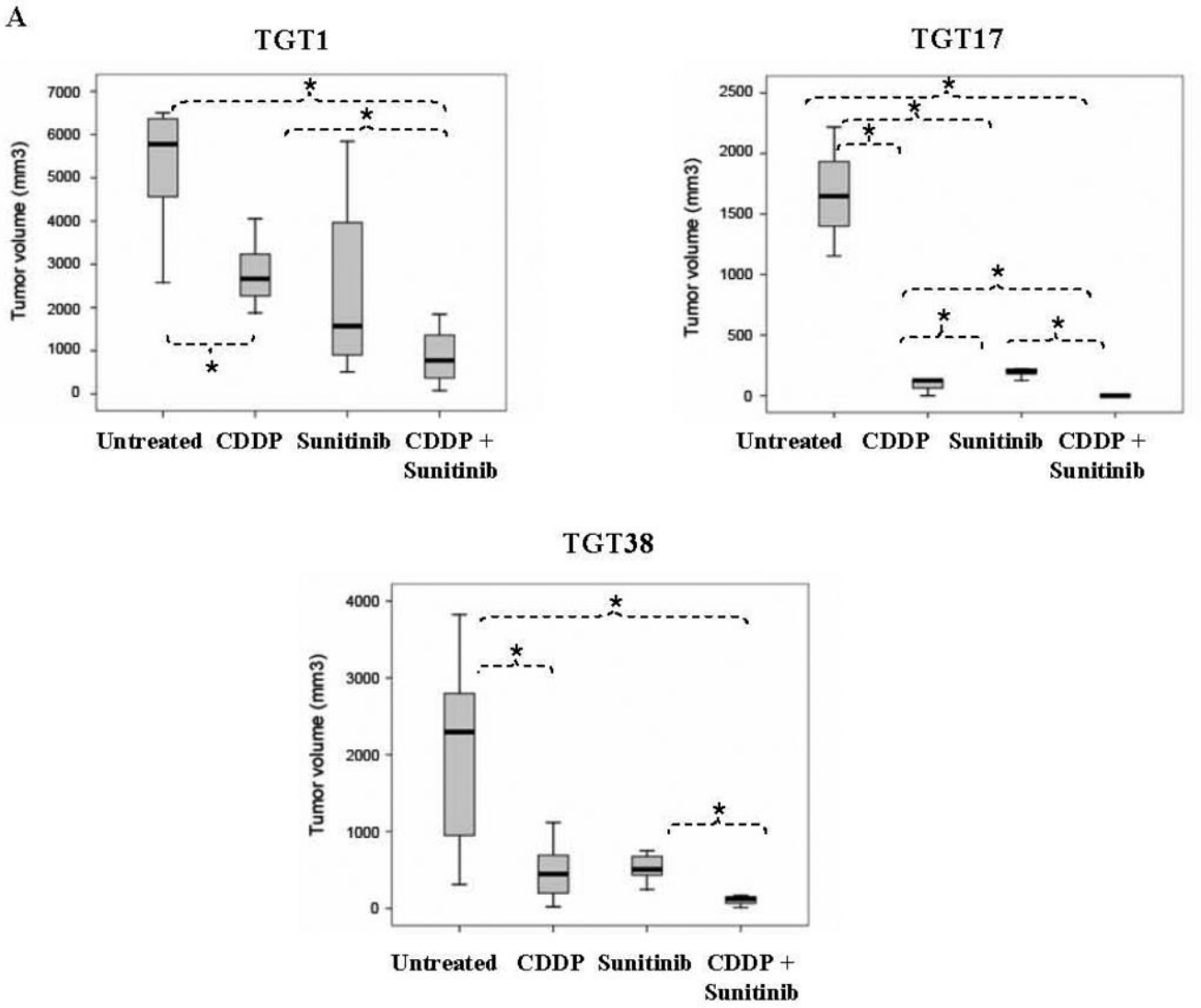
A
TGT1
Tumor volume (mm3)
7000
6000
5000
4000
3000
2000
1000
0
Untreated
CDDP
Sunitinib
CDDP + Sunitinib
TGT17
Tumor volume (mm3)
2500
2000
1500
1000
500
0
Untreated
CDDP
Sunitinib
CDDP + Sunitinib
TGT38
Tumor volume (mm3)
4000
3000
2000
1000
0
Untreated
CDDP
Sunitinib
CDDP + Sunitinib

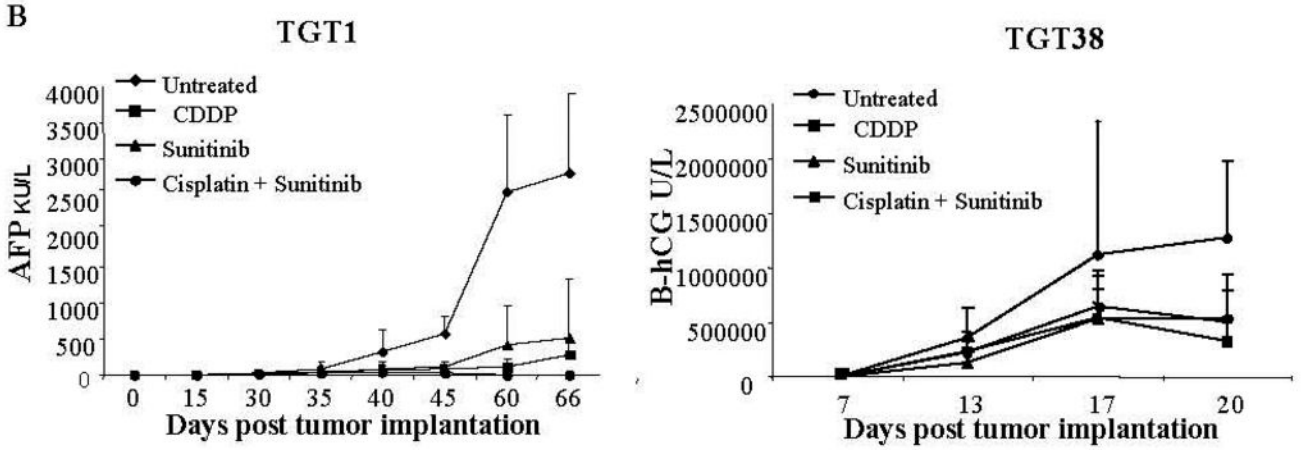
B
TGT1
Untreated
CDDP
Sunitinib
Cisplatin + Sunitinib
AFP KU/L
4000
3500
3000
2500
2000
1500
1000
500
0
0
15
30
35
40
45
60
66
Days post tumor implantation
TGT38
Untreated
CDDP
Sunitinib
Cisplatin + Sunitinib
B-hCG U/L
2500000
2000000
1500000
1000000
500000
0
7
13
17
20
Days post tumor implantation

Fig. 3

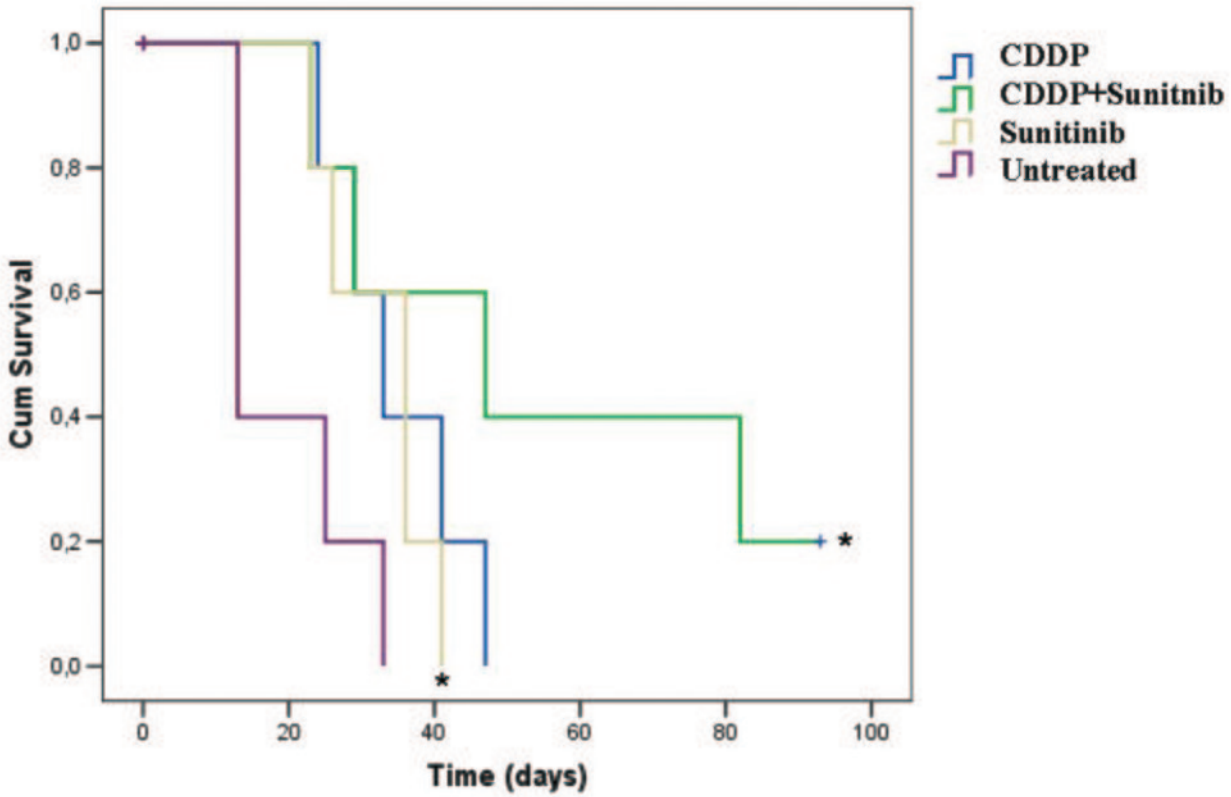
1,0
0,8
0,6
0,4
0,2
0,0
Cum Survival
0
20
40
60
80
100
Time (days)
CDDP
CDDP+Sunitnib
Sunitinib
Untreated

Fig. 4

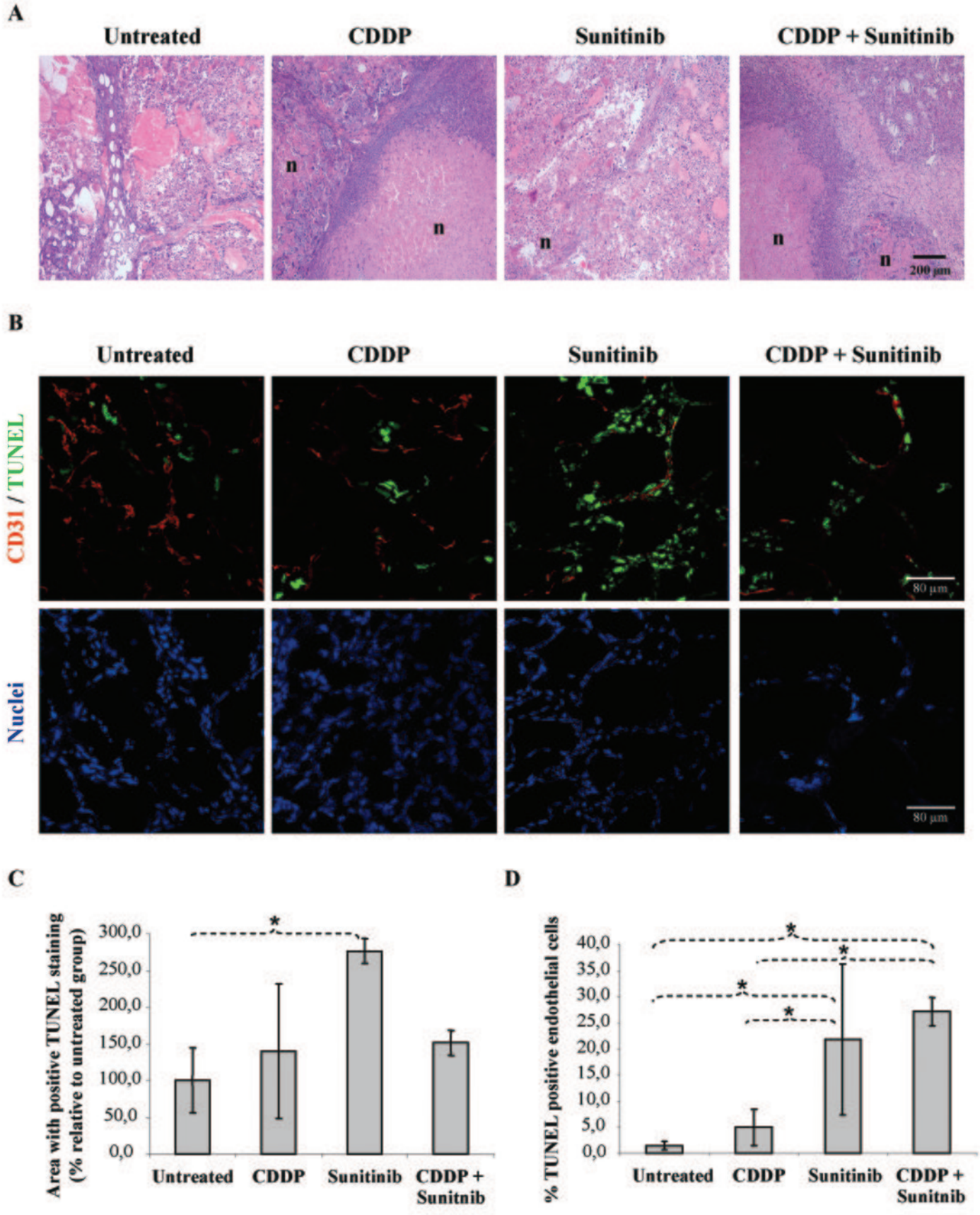
A
Untreated
CDDP
Sunitinib
CDDP + Sunitinib
n
200 µm
B
Untreated
CDDP
Sunitinib
CDDP + Sunitinib
CD31 / TUNEL
Nuclei
80 µm
C
Area with positive TUNEL staining (% relative to untreated group)
300,0
250,0
200,0
150,0
100,0
50,0
0,0
Untreated
CDDP
Sunitinib
CDDP + Sunitnib
D
% TUNEL positive endothelial cells
40,0
35,0
30,0
25,0
20,0
15,0
10,0
5,0
0,0
Untreated
CDDP
Sunitinib
CDDP + Sunitnib

Fig. 5

A

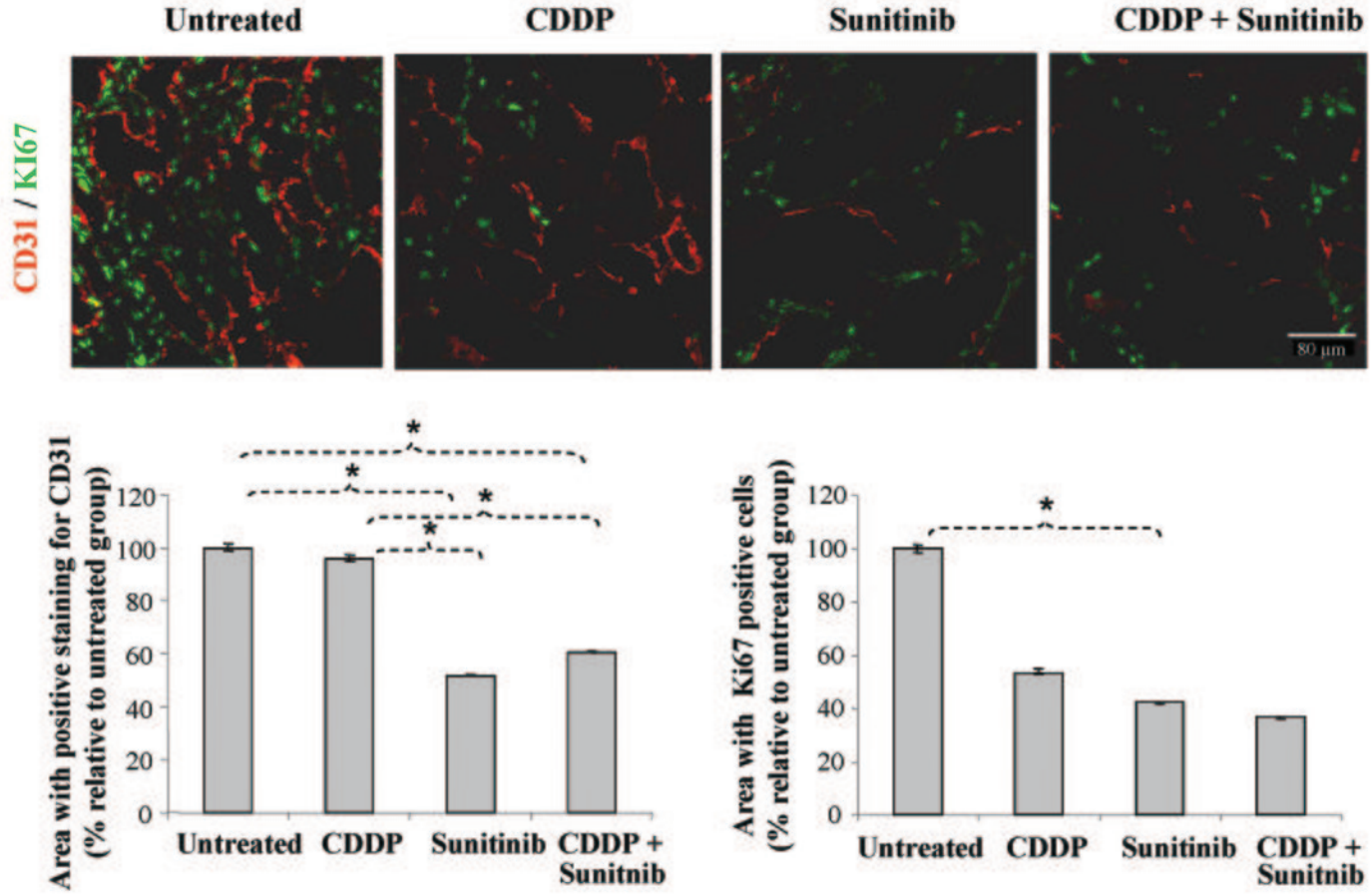
Untreated
CDDP
Sunitinib
CDDP + Sunitinib
CD31 / KI67
80 µm
Area with positive staining for CD31 (% relative to untreated group)
120
100
80
60
40
20
0
Untreated
CDDP
Sunitinib
CDDP + Sunitnib
Area with Ki67 positive cells (% relative to untreated group)
120
100
80
60
40
20
0
Untreated
CDDP
Sunitinib
CDDP + Sunitnib

B

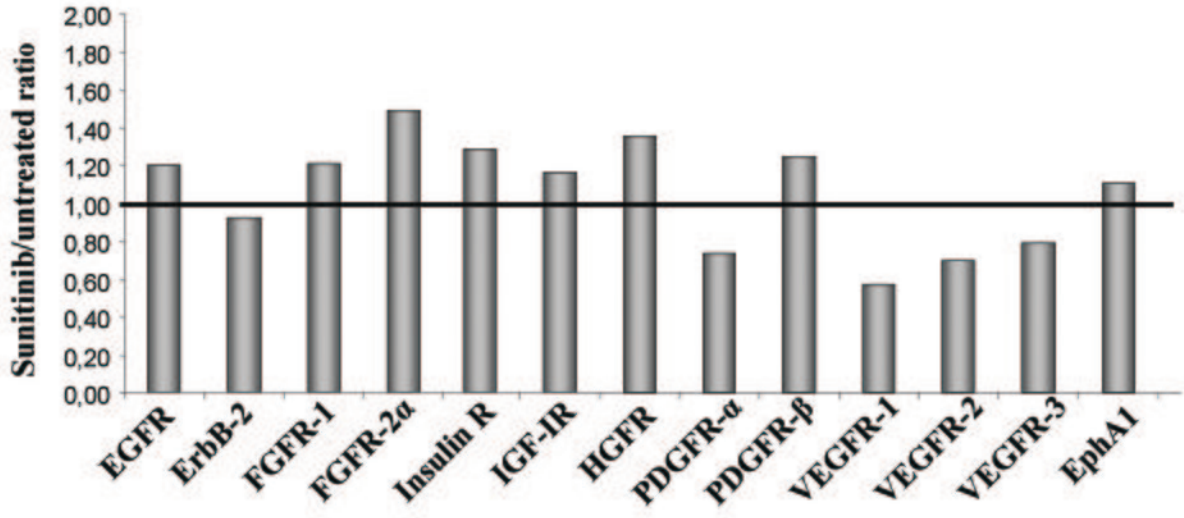
Sunitinib/untreated ratio
2,00
1,80
1,60
1,40
1,20
1,00
0,80
0,60
0,40
0,20
0,00
EGFR
ErbB-2
FGFR-1
FGFR-2α
Insulin R
IGF-IR
HGFR
PDGFR-α
PDGFR-β
VEGFR-1
VEGFR-2
VEGFR-3
EphA1

Fig. 6

A

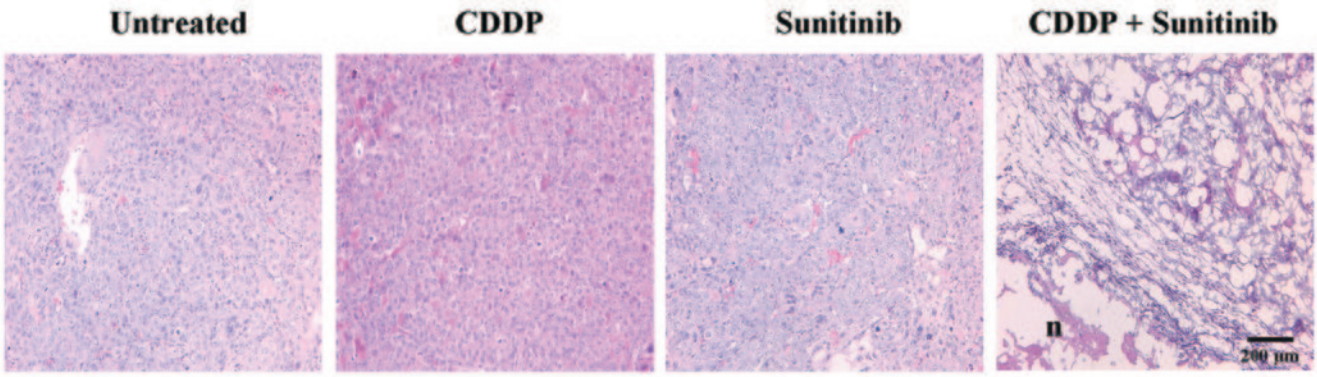
Untreated
CDDP
Sunitinib
CDDP + Sunitinib
n
200 µm

B

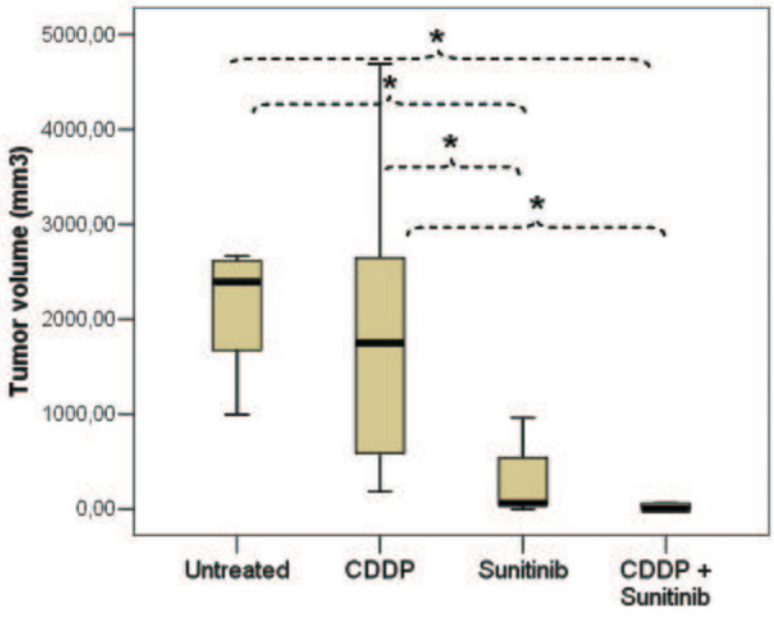
Tumor volume (mm3)
5000,00
4000,00
3000,00
2000,00
1000,00
0,00
*
*
*
*
Untreated
CDDP
Sunitinib
CDDP + Sunitinib